Robust Maneuver Load Alleviation via LPV Aeroservoelastic Model

Hongkun Li[*], Rui Huang, Yonghui Zhao and Haiyan Hu
[*] *State Key Laboratory of Mechanics and Control of Mechanical Structures,*
Nanjing University of Aeronautics and Astronautics,
210016 Nanjing, People's Republic of China

Abstract. In this paper, the aeroservoelastic (ASE) model is constructed in state-space to deal with the maneuver load of a high-performance military aircraft. Then a model interpolation method is demonstrated for constructing linear parameter-varing (LPV) ASE model. Here the plant state-space matrices are assumed to depend on the Mach number. The controller design is based on robust H_∞ control theory. Finally, a series of numerical simulations is tested to verify the control effect. The studies demonstrate that the robust controller can realize maneuver load alleviation (MLA) in a wide range of Mach numbers.

Introduction

In the design process of modern aircraft, the load alleviation technique gains increasing attention over the past decades. The use of such technique can reduce additional structural loads due to both wind gusts and aircraft maneuvers to get decreased structure weight, extended structure life and enhanced flight performance. For high-performance military aircrafts, only MLA is taken into consideration as ride comfort is not a concern. The MLA techniques have been studied since the 1970s [1-6]. For example, Anderson et al. synthesized the classic-control-based longitudinal flight control system for an F-4E model to realize MLA [1]. Woods-Vedler et al. presented a systematic approach for designing rolling MLA control laws and demonstrated a rolling MLA system on the wind-tunnel model of an Active Flexible Wing [3]. Gaulocher et al. used the model predictive control (MPC) to attenuate the structure response of sudden roll maneuvers [4]. Paletta designed a maneuver load control system for longitudinal maneuvers of a High Altitude Performance Demonstrator, and reduced the wing-root bending moment by approximately 20% while following the desired normal load factor law [5]. These controllers mostly could not deal with a wide range of flight conditions, such as Mach numbers and dynamic pressure. The control laws have to be updated during an actual flight. To realize an adaptive controller, an LPV model is essential for accuracy prediction of aeroelastic (AE) behavior in a wide range of flight conditions, and hence, a robust ASE controller can be synthesized.

Aeroservoelastic Model

The dynamic equation of the aeroelastic system of concern in generalized coordinates yields [9]

$$\mathbf{M}_s\ddot{\boldsymbol{\xi}}+\mathbf{C}_s\dot{\boldsymbol{\xi}}+\mathbf{K}_s\boldsymbol{\xi}+q_\infty\mathbf{Q}_s(p)\boldsymbol{\xi}=-(\mathbf{M}_c\ddot{\boldsymbol{\delta}}_c+q_\infty\mathbf{Q}_c(p)\boldsymbol{\delta}_c)+\mathbf{P} \tag{1}$$

where p is the nondimensional Laplace variable, $\mathbf{M}_s,\mathbf{C}_s$ and $\mathbf{K}_s$ are the generalized mass matrix, damping matrix and stiffness matrix, respectively. $\mathbf{M}_c$ is the coupling mass matrix between the control and structural modes, $\boldsymbol{\delta}_c$ is the vector of the control surface deflections, $\mathbf{Q}_s$ and $\mathbf{Q}_c$ are the matrices of generalized unsteady aerodynamic-force coefficients associated with the structural and control modes, respectively, and $\mathbf{P}$ represents the vector of gravitational forces. $\boldsymbol{\xi}$ is the vector of generalized coordinates of the finite element model of the structure and takes the following form

$$\boldsymbol{\xi}=\begin{Bmatrix}\mathbf{x}_q\\\mathbf{x}_e\end{Bmatrix} \tag{2}$$

where $\mathbf{x}_q$ and $\mathbf{x}_e$ are the vectors of generalized coordinates of rigid-body modes and elastic modes, respectively. The equation is combined by $\boldsymbol{\delta}_c$, $\boldsymbol{\xi}$ in time domain and $\mathbf{Q}_s$, $\mathbf{Q}_c$ in Laplace domain.

After the minimum-state approximation is applied to the matrices of aerodynamic force coefficients and the actuators modelled, the dynamic equation of the aeroelastic system can be recast in the state space as follows [9]

$$\dot{\mathbf{x}}_p=\mathbf{A}_p\mathbf{x}_p+\mathbf{B}_p\mathbf{u}_p \tag{3}$$

where

$$\mathbf{x}_p=\begin{Bmatrix}\mathbf{x}_{ae}\\\mathbf{x}_{ac}\end{Bmatrix},\mathbf{A}_p=\begin{bmatrix}\mathbf{A}_{ae}&\mathbf{B}_{ae}\\\mathbf{0}&\mathbf{A}_{ac}\end{bmatrix},\mathbf{B}_p=\begin{bmatrix}\mathbf{0}\\\mathbf{B}_{ac}\end{bmatrix},\mathbf{u}_p=\mathbf{u}_{ac} \tag{4}$$

and

$$\mathbf{x}_{ae}=\begin{Bmatrix}\boldsymbol{\xi}\\\dot{\boldsymbol{\xi}}\\\mathbf{x}_a\end{Bmatrix},\quad\mathbf{u}_{ae}=\begin{Bmatrix}\boldsymbol{\delta}_c\\\dot{\boldsymbol{\delta}}_c\\\ddot{\boldsymbol{\delta}}_c\end{Bmatrix},\dot{\mathbf{x}}_{ac_i}=\begin{bmatrix}0&1&0\\0&0&1\\-a_{i3}&-a_{i2}&-a_{i1}\end{bmatrix}\mathbf{x}_{ac_i}+\begin{Bmatrix}0\\0\\a_{i3}\end{Bmatrix}u_{ac_i},\mathbf{x}_{ac_i}=\begin{Bmatrix}\delta_{ci}\\\dot{\delta}_{ci}\\\ddot{\delta}_{ci}\end{Bmatrix} \tag{5}$$

Here, $\mathbf{x}_a$ is the vector of aerodynamic state, a_{i1}, a_{i2}, a_{i3} is parameters from transfer function of the actuator driving the ith control surface, which is given by

$$\frac{\delta_{c_i}(s)}{u_{ac_i}(s)} = \frac{a_{i3}}{s^3 + a_{i1}s^2 + a_{i2}s + a_{i3}} \tag{6}$$

where u_{ac_i} is the servo-commanded control surface deflection.

The output equation becomes

$$\mathbf{y}_p = \mathbf{C}_p \mathbf{x}_p \tag{7}$$

where

$$\mathbf{C}_p = \begin{bmatrix} \mathbf{C}_{ae} & \mathbf{D}_{ae} \end{bmatrix} \tag{8}$$

For the transient maneuver analysis, it is more convenient to transform the rigid-body modes of the structure into the airframe states. The transformation is shown as follows.

In the principle axes, six generalized coordinates for the rigid-body modes of the structure is

$$\mathbf{x}_q = \{ q_1 \quad q_2 \quad q_3 \quad q_4 \quad q_5 \quad q_6 \}^{\mathrm{T}} \tag{9}$$

which are generated from the finite element model.

The transformation of $\mathbf{x}_q$ to $\boldsymbol{\xi}_R$ in the body axes reads

$$\mathbf{x}_q = \mathbf{R}_p^{-1} \mathbf{R}_b \boldsymbol{\xi}_R \tag{10}$$

where $\mathbf{R}_p$ is the rigid-body modal matrix in the principle axes, $\mathbf{R}_b$ is the rigid-body modal matrix in the body axes defined at the center of gravity, and

$$\boldsymbol{\xi}_R = \{ T_x \quad T_y \quad T_z \quad R_x \quad R_y \quad R_z \}^{\mathrm{T}} \tag{11}$$

The airframe axes are written as

$$\boldsymbol{\xi}_{AS} = \{ x \quad y \quad u \quad \beta \quad h \quad p \quad \alpha \quad r \quad \theta \quad \phi \quad q \quad \psi \}^{\mathrm{T}} \tag{12}$$

where x is the perturbed forward position, y is the perturbed lateral position, u is the perturbed forward velocity, β is the perturbed side slip angle, h is the perturbed altitude, p is the perturbed roll rate, α is the perturbed angle of attack, r is the perturbed yaw rate, θ is the perturbed Euler pitch angle, ϕ is the perturbed Euler roll angle, q is the perturbed pitch rate and ψ is the perturbed Euler azimuth angle. In this paper, only longitudinal flights are taken into consideration. Thus, for a symmetric flight condition, the transformation yields

$$\begin{Bmatrix} T_x \\ T_z \\ R_y \\ \dot{T}_x \\ \dot{T}_z \\ \dot{R}_y \end{Bmatrix} = \begin{bmatrix} -1 & 0 & 0 & 0 & 0 & 0 \\ 0 & 0 & 1 & 0 & 0 & 0 \\ 0 & 0 & 0 & 0 & 1 & 0 \\ 0 & -1 & 0 & 0 & 0 & 0 \\ 0 & 0 & 0 & -V_\infty & V_\infty & 0 \\ 0 & 0 & 0 & 0 & 0 & 1 \end{bmatrix} \begin{Bmatrix} x \\ u \\ h \\ \alpha \\ \theta \\ q \end{Bmatrix} \tag{13}$$

The final dynamic equation of system in the state-space form after the transformation reads

$$\begin{Bmatrix} \dot{\boldsymbol{\xi}}_{AS} \\ \dot{\mathbf{x}}_\xi \end{Bmatrix} = \bar{\mathbf{A}}_p \begin{Bmatrix} \boldsymbol{\xi}_{AS} \\ \mathbf{x}_\xi \end{Bmatrix} + \bar{\mathbf{B}}_p \mathbf{u}_p \tag{14}$$

where

$$\mathbf{x}_\xi = \begin{Bmatrix} \mathbf{x}_e \\ \dot{\mathbf{x}}_e \\ \mathbf{x}_a \\ \mathbf{x}_{ac} \end{Bmatrix} \tag{15}$$

Here, $\bar{\mathbf{A}}_p$ and $\bar{\mathbf{B}}_p$ are the system matrices resulting from the transformation. Written in intuitive form,

$$\begin{bmatrix} \dot{\bar{\mathbf{x}}}_p \\ \mathbf{y}_p \end{bmatrix} = \begin{bmatrix} \bar{\mathbf{A}}_p & \bar{\mathbf{B}}_p \\ \mathbf{C}_p & \mathbf{0} \end{bmatrix} \begin{bmatrix} \bar{\mathbf{x}}_p \\ \mathbf{u}_p \end{bmatrix} \tag{16}$$

Linear Parameter-Varying Aeroservoelastic Models

In this paper, a fighter symmetric climb maneuver is modelled. The aerodynamic mesh is shown in Fig. 1. The inputs of the ASE plant are deflections of a pair of stabilators and a pair of ailerons, and the outputs are the fighter's load factor and wing-root bending moment.
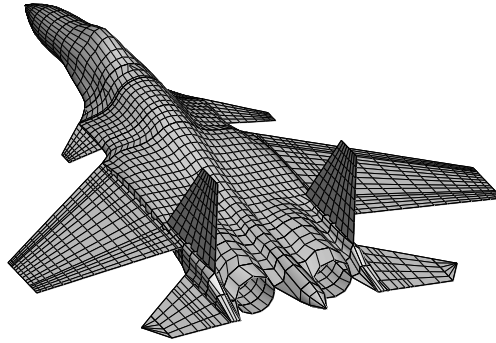
Fig. 1 Aerodynamic mesh of the fighter

LPV models are state-space models with the state-space matrices described in the functions of time-varying parameters [8],

$$\begin{bmatrix} \dot{\bar{\mathbf{x}}}_p(t) \\ \mathbf{y}_p(t) \end{bmatrix} = \begin{bmatrix} \bar{\mathbf{A}}_p(\rho) & \bar{\mathbf{B}}_p(\rho) \\ \mathbf{C}_p(\rho) & \mathbf{0} \end{bmatrix} \begin{bmatrix} \bar{\mathbf{x}}_p(t) \\ \mathbf{u}_p(t) \end{bmatrix} \tag{17}$$

Where ρ is the vector of measurable parameters, such as Mach number, altitude and dynamic pressure. In this paper, the LPV ASE model is represented by the linearization on a gridded domain. The parameter of the gridded domain is Mach number, range from 0.3 to 0.5 in 0.02 Mach increments. Thus a set of 11 models are generated on grid points of the 1D parameter space, as shown in Fig. 2.
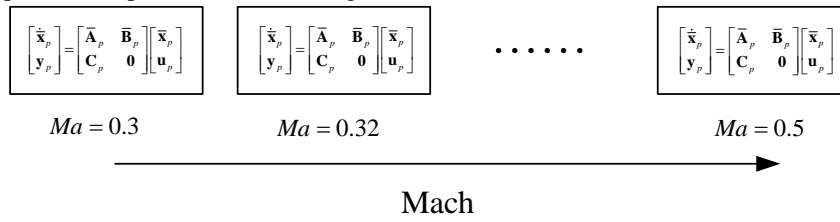
Fig. 2 Grid-based LPV

The interpolation is using quadratic polynomial fitting. The comparison of the bode plots between the ASE models obtained by generation on 0.53 Mach and LPV model interpolation is shown in Fig. 3.
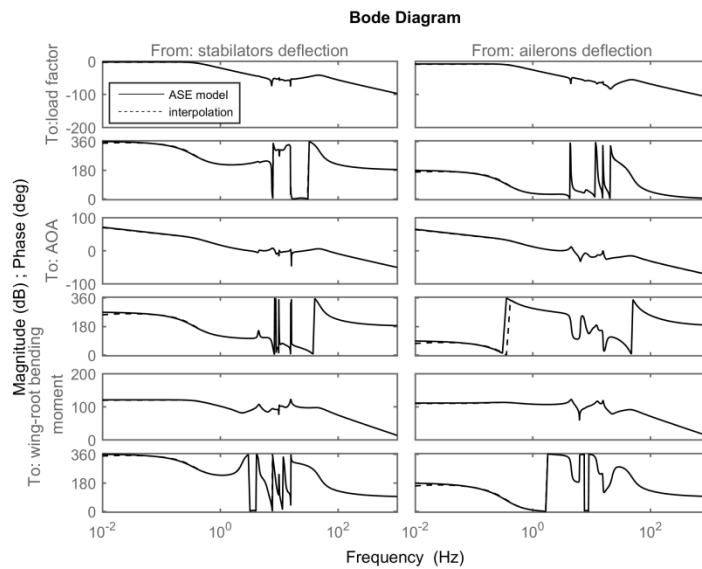
Fig. 3 Comparison of the bode plots between the generated ASE models and interpolation

Robust Controller Design

To synthesize the robust controller, linear fractional transformation (LFT) is necessary. LFT is a method to deal with the uncertainty of the model, for the LPV model discussed in this paper, the uncertainty of the Mach number can be modelled as follow.

Assume the system matrix of ASE model can be written as quadratic polynomial function of parameter ρ_0, for example,

$$\bar{\mathbf{A}}_p(\rho_0) = Ka_1\rho_0{}^2 + Ka_2\rho_0 + Ka_3 \tag{18}$$

then

$$\bar{\mathbf{A}}_p(\rho_0 + \Delta\rho\delta) = Ka_1\left(\rho_0 + \Delta\rho\delta\right)^2 + Ka_2\left(\rho_0 + \Delta\rho\delta\right) + Ka_3 \tag{19}$$

where $\Delta\rho$ is the maximum amplitude of the uncertainty parameter, $\delta \in [-1,1]$ is the nondimensional disturbance, then the effects of δ is

$$\bar{\mathbf{A}}_p = \bar{\mathbf{A}}_p(\rho_0) + \left(2Ka_1\rho_0\Delta\rho + Ka_2\Delta\rho\right)\delta + \left(Ka_1\Delta\rho^2\right)\delta^2 \tag{20}$$

which can be written in a short form

$$\bar{\mathbf{A}}_p = \bar{\mathbf{A}}_p^n + a_1\delta + a_2\delta^2 \tag{21}$$

where

$$\bar{\mathbf{A}}_p^n = \bar{\mathbf{A}}_p(\rho_0), a_1 = 2Ka_1\rho_0\Delta\rho + Ka_2\Delta\rho, a_2 = Ka_1\Delta\rho^2 \tag{22}$$

rewrite Equation (21) in LFT form as follows

$$\bar{\mathbf{A}}_p = F_l(\mathbf{M},\mathbf{\Delta}) = \mathbf{M}_{11} + \mathbf{M}_{12}\mathbf{\Delta}(\mathbf{I} - \mathbf{M}_{22}\mathbf{\Delta})^{-1}\mathbf{M}_{21} \tag{23}$$

where

$$\mathbf{M}_{11} = \bar{\mathbf{A}}_p^n, \mathbf{M}_{12} = \begin{bmatrix} a_1 & a_2 \end{bmatrix}, \mathbf{M}_{21} = \begin{bmatrix} \mathbf{I}_{n_p} \\ 0 \end{bmatrix}, \mathbf{M}_{22} = \begin{bmatrix} 0 & 0 \\ \mathbf{I}_{n_p} & 0 \end{bmatrix}, \mathbf{\Delta} = \mathbf{I}_{2n_p}\delta \tag{24}$$

Similarly, the LFT form of C_p can be written as

$$\mathbf{C}_p = F_l(\mathbf{Q},\mathbf{\Delta}) = \mathbf{Q}_{11} + \mathbf{Q}_{12}\mathbf{\Delta}(\mathbf{I} - \mathbf{Q}_{22}\mathbf{\Delta})^{-1}\mathbf{Q}_{21} \tag{25}$$

where

$$\mathbf{Q}_{11} = \mathbf{C}_p^n, \mathbf{Q}_{12} = \begin{bmatrix} c_1 & c_2 \end{bmatrix}, \mathbf{Q}_{21} = \begin{bmatrix} \mathbf{I}_{n_p} \\ 0 \end{bmatrix}, \mathbf{Q}_{22} = \begin{bmatrix} 0 & 0 \\ \mathbf{I}_{n_p} & 0 \end{bmatrix}, \mathbf{\Delta} = \mathbf{I}_{2n_p}\delta \tag{26}$$

$$c_1 = 2Kc_1\rho_0\Delta\rho + Kc_2\Delta\rho, c_2 = Kc_1\Delta\rho^2$$

Then the ASE model with uncertainty is

$$\dot{\bar{\mathbf{x}}}_p = \bar{\mathbf{A}}_p^n\bar{\mathbf{x}}_p + \begin{bmatrix} a_1 & a_2 \end{bmatrix}\mathbf{w} + \bar{\mathbf{B}}_p\mathbf{u}_p$$
$$\mathbf{z} = \begin{bmatrix} \mathbf{I}_{n_p} \\ 0 \end{bmatrix}\bar{\mathbf{x}}_p + \begin{bmatrix} 0 & 0 \\ \mathbf{I}_{n_p} & 0 \end{bmatrix}\mathbf{w} \tag{27}$$
$$\mathbf{y} = \mathbf{C}_p^n\bar{\mathbf{x}}_p + \begin{bmatrix} c_1 & c_2 \end{bmatrix}\mathbf{w}$$

written as

$$\dot{\bar{\mathbf{x}}}_p = \mathbf{A}\mathbf{x}_p + \mathbf{B}_1\mathbf{w} + \mathbf{B}_2\mathbf{u}_p$$
$$\mathbf{z} = \mathbf{C}_1\mathbf{x}_p + \mathbf{D}_{11}\mathbf{w} + \mathbf{D}_{12}\mathbf{u}_p \tag{28}$$
$$\mathbf{y} = \mathbf{C}_2\mathbf{x}_p + \mathbf{D}_{21}\mathbf{w} + \mathbf{D}_{22}\mathbf{u}_p$$

The construct of robust control system is shown in Fig. 4.
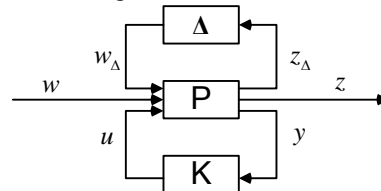
Fig. 4 LPV plant with LPV controller

In this paper, the range of the Mach number is from 0.3 to 0.5, with the nominal value of the LFT-based LPV model set to be 0.48.

The synthesis of the MLA system, a 2-degree-of-freedom (2DOF) controller is constructed with Matlab Robust Control Toolbox, the block-diagram of the closed-loop system is shown in [10]. The ideal model M is a modified ASE model of $Mach = 0.5$ which has the same load factor response and a small response of wing-root bending moment.

Results and Discussion

The open-loop maneuver is achieved by the deflection of the stabilators, as shown in Fig. 5. The closed-loop responses at nominal Mach number 0.48 is shown in Fig. 6. The closed-loop response of load factor tracks well with the open-loop one while the wing-root bending moment has been alleviated by 38%. The closed-loop responses at $Ma = 0.5$, $Ma = 0.4$ and $Ma = 0.3$ (the maximum, the middle and the minimum Mach number) is shown in Fig. 7, Fig. 8 and Fig. 9, respectively. The tracking of the load factor works well at $Ma = 0.5$ and $Ma = 0.4$, however, at $Ma = 0.3$, load factor response can't track the ideal model well, and the alleviation of the wing-root bending moment also drops to 25%.
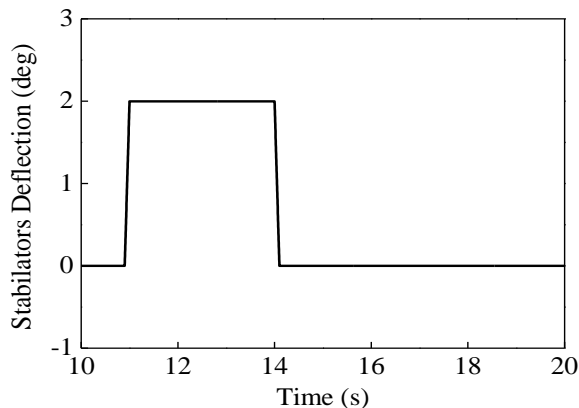
Fig. 5 Open-loop stabilators deflection
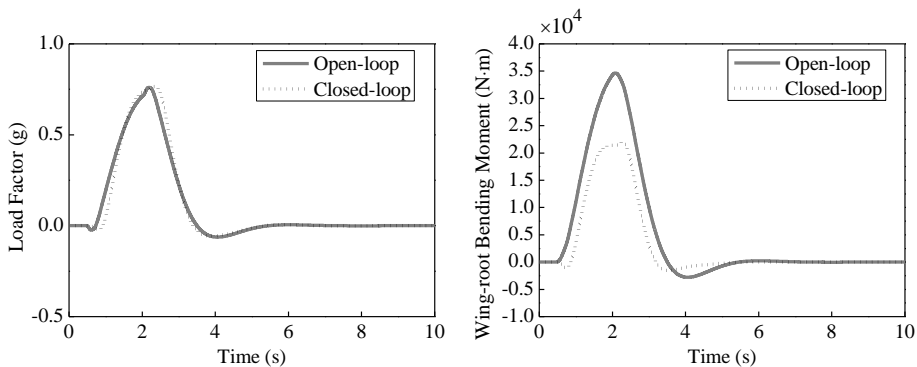
Fig. 6 Closed-loop responses at $Ma = 0.48$
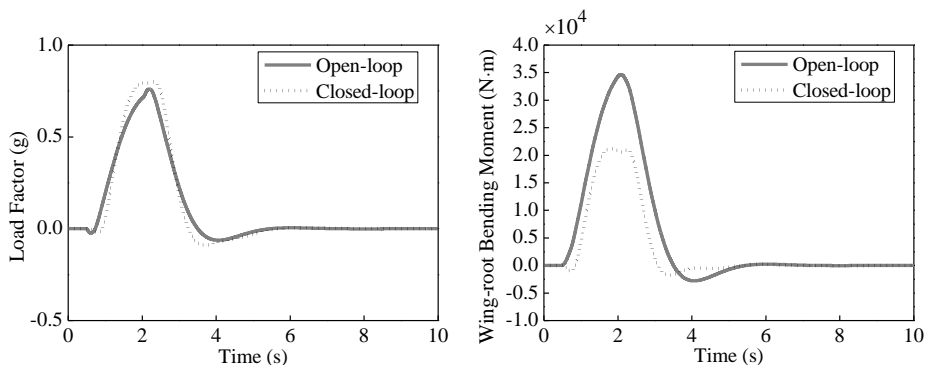
Fig. 7 Closed-loop responses at $Ma = 0.5$
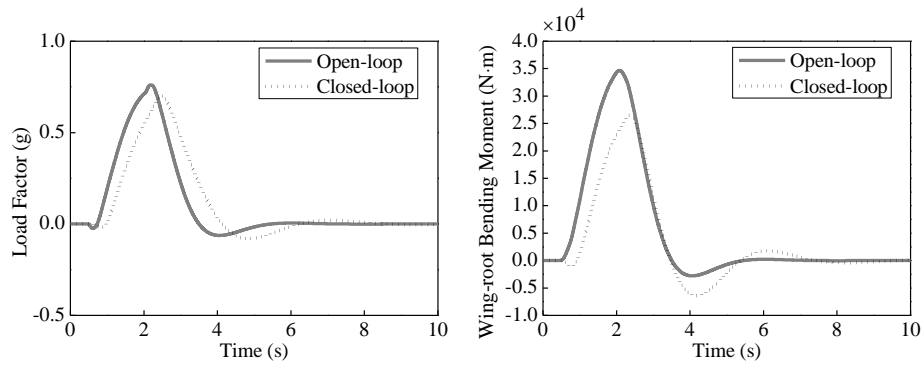
Fig. 8 Closed-loop responses at $Ma = 0.4$
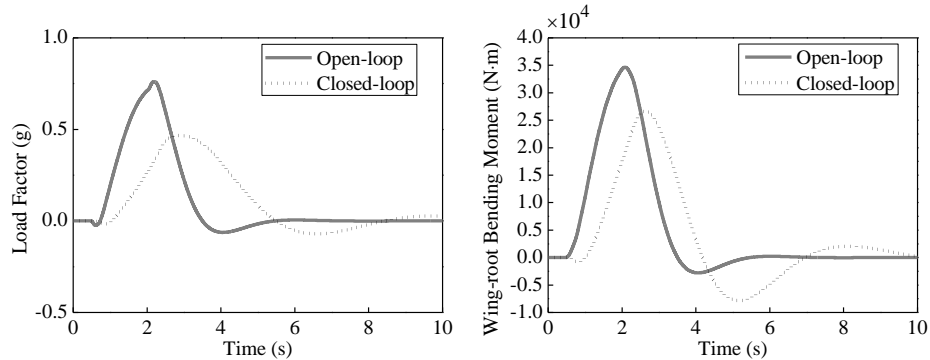
Fig. 9 Closed-loop responses at $Ma = 0.3$

The numerical simulations demonstrate the feasibility of the robust maneuver load alleviation based on LPV ASE model. The ASE model of a wide Mach number range can be calculated by interpolation of the LPV model with high accuracy. Moreover, the 2DOF H_∞ controller can be synthesized to realized the alleviation of maneuver load. However, the performance of the load factor tracking remains to be improved.

Acknowledgements

References

[1]   Anderson, D.C., Berger, R. L., and Hess Jr, J. R., "Maneuver Load Control and Relaxed Static Stability Applied to a Contemporary Fighter Aircraft," *Journal of Aircraft*, Vol. 10, No. 2, 1973, pp. 112-120.
[2]   Mukhopadhyay, V., "Flutter Suppression Digital Control Law Design and Testing for the AFW Wind Tunnel Model," NASA TM 107652, Hampton, VA, 1992.
[3]   Woods-Vedler, J. A., Pototzky, A., and Hoadley, S., "Rolling Maneuver Load Alleviation Using Active Control," *Journal of Aircraft*, Vol. 32, No. 1, 1995, pp. 68–76.
[4]   Gaulocher, S. L., Roos, C., and Cumer, C., "Aircraft Load Alleviation During Maneuvers Using Optimal Control Surface Combinations," *Journal of Guidance, Control, and Dynamics*, Vol. 30, No. 2, 2007, pp. 591–600.
[5]   Paletta, N., Belardo, M., and Pecora, M., "Load Alleviation on a Joined Wing Unmanned Aircraft," *Journal of Aircraft*, Vol. 47, No. 6, 2010, pp. 2005–2016.
[6]   Khatri, A. K., Singh, J., and Sinha, N. K., "Accessible regions for controlled aircraft maneuvering," *Journal of Guidance, Control, and Dynamics*, Vol. 36, No .6, 2013, pp. 1829-1834.
[7]   Baldelli, D. H., Chen, P. C., and Panza, J., "Unified Aeroelastic and Flight Dynamic Formulation via Rational Function Approximations," *Journal of Aircraft*, Vol. 43, No. 3, 2006, pp. 763–772.
[8]   Wang, Yi, et al. "Model Order Reduction of Aeroservoelastic Model of Flexible Aircraft." *57th AIAA/ASCE/AHS/ASC Structures, Structural Dynamics, and Materials Conference*. 2016.
[9]   Baldelli, D. H., Chen, P. C., and Panza, J., "Unified Aeroelastic and Flight Dynamic Formulation via Rational Function Approximations," *Journal of Aircraft*, Vol. 43, No. 3, 2006, pp. 763–772.
[10] Gu, Da-Wei, Petko Petkov, and Mihail M. Konstantinov. *Robust control design with MATLAB®*. Springer Science & Business Media, 2014.